Year : 2016

Low Dose Photodynamic Therapy Enhances the Distribution and Efficiency of Lipoplatin in a Rodent Model of Mesothelioma: Insights of using Intravital Microscopy

WANG Xingyu

WANG Xingyu, 2016, Low Dose Photodynamic Therapy Enhances the Distribution and Efficiency of Lipoplatin in a Rodent Model of Mesothelioma: Insights of using Intravital Microscopy

Originally published at : Thesis, University of Lausanne

Posted at the University of Lausanne Open Archive http://serval.unil.ch
Document URN : urn:nbn:ch:serval-BIB_7402C30228AD2

UNIVERSITE DE LAUSANNE - FACULTE DE BIOLOGIE ET DE MEDECINE

Département des Services de Chirurgie et d'Anesthésiologie
Service de Chirurgie Thoracique

Low Dose Photodynamic Therapy Enhances the Distribution and Efficiency of Lipoplatin in a Rodent Model of Mesothelioma: Insights of using Intravital Microscopy

THESE

préparée sous la direction du Professeur Hans-Beat Ris
(avec la co-direction du Docteur Jean Yannis Perentes)

et présentée à la Faculté de biologie et de médecine de
l'Université de Lausanne pour l'obtention du grade de

DOCTEUR EN MEDECINE

par

Xingyu WANG

Médecin diplômé du Chine

Originaire de Wuhan Chine

Lausanne

2016

UNIVERSITE DE LAUSANNE - FACULTE DE BIOLOGIE ET DE MEDECINE

Département des Services de Chirurgie et d'Anesthésiologie
Service de Chirurgie Thoracique

Low Dose Photodynamic Therapy Enhances the Distribution and Efficiency of Lipoplatin in a Rodent Model of Mesothelioma: Insights of using Intravital Microscopy

THESE

préparée sous la direction du Professeur Hans-Beat Ris
(avec la co-direction du Docteur Jean Yannis Perentes)

et présentée à la Faculté de biologie et de médecine de
l'Université de Lausanne pour l'obtention du grade de

DOCTEUR EN MEDECINE

par

Xingyu WANG

Médecin diplômé du Chine

Originaire de Wuhan Chine

Lausanne

2016

UNIL | Université de Lausanne

Faculté de biologie et de médecine

Ecole Doctorale
Doctorat en médecine

Imprimatur

Vu le rapport présenté par le jury d'examen, composé de

Directeur de thèse	*Monsieur le Professeur* **Hans-Beat Ris**
Co-Directeur de thèse	*Monsieur le Docteur* **Jean Perentes**
Expert	*Monsieur le Professeur* **Patrice Jichlinski**
Directeur de l'Ecole doctorale	*Monsieur le Professeur* **Niko Geldner**

la Commission MD de l'Ecole doctorale autorise l'impression de la thèse de

Monsieur Xingyu WANG

intitulée

Low dose photodynamic therapy enhances the distribution and efficiency of Lipoplatin in a rodent model of mesothelioma: insights of using intravital microscopy

Lausanne, le 19 avril 2016

pour Le Doyen
de la Faculté de Biologie et de Médecine

Monsieur le Professeur John Prior
Vice-Directeur de l'Ecole doctorale

Amélioration de la distribution de chimiothérapie par photothérapie dynamique intracavitaire pour la prise en charge des épanchements pleuraux malins

Xingyu Wang, Dr Hans-Beat Ris, Dr JY Perentes

Les épanchements pleuraux malins sont une pathologie difficile à gérer tant pour le patient en raison de la symptomatologie de dyspnée qu'ils entrainent que pour les soignants en raison de l'absence de thérapies satisfaisantes. La prise en charge de cette pathologie consiste, en général, en la combinaison d'une chimiothérapie palliative à une pleurodèse chirurgicale.

Une des nombreuses raisons de la non-réponse tumorale à la chimiothérapie standard peut être expliquée par la vascularisation anormale des tumeurs. Ces dernières sont en effet dépendantes de la néo-angiogénése qui cause la création de réseaux vasculaires hautement perméables. Ceci résulte en une pression interstitielle intra-tumorale et des forces de convection fortement diminuées limitant le transport de molécules entre le milieu intra- et extracellulaire.

Dans le passé, nous avons pu démontrer que le prétraitement du lit vasculaire tumoral par photothérapie dynamique à faible dose (L-PDT) pouvait moduler la vascularisation tumorale de façon à faire baisser la pression interstitielle tout en maintenant un flux de perfusion constant. Ceci résultait en une augmentation significative de la quantité et de l'homogénéité de la distribution de chimiothérapie dans des tumeurs solides qui prédit une meilleure réponse tumorale

Dans ce travail de thèse, nous avons, dans un premier temps, confirmé et affiné les résultats préliminaires de modulation vasculaire tumorale par L-PDT. En combinant des modèles de carcinose pleurale à la microscopie intravitale, nous avons pu définir les conditions optimales de « fluence » et « fluence rate » de la L-PDT afin d'obtenir la meilleure réponse vasculaire et le meilleur transport subséquent de chimiothérapie intratumorale. Nous avons ensuite confirmé qu'une meilleure distribution de chimiothérapie résultait en une meilleure réponse tumorale et avons validé ce concept dans 3 modèles tumoraux couvrant les épanchements carcinomateux les plus fréquents chez l'humain. Finalement, nous avons testé la faisabilité de l'approche de L-PDT intracavitaire par thoracoscopie avec monitoring de fluence au cours du temps et effectué une étude toxicologique dans un modèle préclinique. Ces travaux ainsi que les précédents ont permis de finaliser une étude clinique de phase I qui validera la faisabilité d'une approche de L-PDT intracavitaire combinée à une chimiothérapie liposomale dans la prise en charge des épanchements pleuraux malins chez l'homme. Cette étude va débuter en janvier 2016 et sera menée par le service de Chirurgie Thoracique du CHUV.

Sur la base des éléments pré-cliniques de ce travail de thèse, la L-PDT intracavitaire permet une modulation du réseau vasculaire tumoral qui est favorable à la distribution subséquente de chimiothérapie. Ceci semble prédire une meilleure réponse tumorale chez l'homme par rapport à l'administration standard d'une chimiothérapie classique et un meilleur potentiel de contrôle tumoral et des symptomes.

Lasers in Surgery and Medicine 47:323–330 (2015)

Fluence Plays a Critical Role on the Subsequent Distribution of Chemotherapy and Tumor Growth Delay in Murine Mesothelioma Xenografts Pre-Treated by Photodynamic Therapy

Yabo Wang, MD, PhD,[1#] Xingyu Wang, MD,[1#] Marie-Aude Le Bitoux,[2] Georges Wagnieres,[3] Hubert Vandenbergh,[3] Michel Gonzalez,[1] Hans-Beat Ris,[1] Jean Y Perentes,[1*#] and Thorsten Krueger[1*#]

[1]*Department of Thoracic and Vascular Surgery, Centre Hospitalier Universitaire Vaudois, Ecole Polytechnique Federale de Lausanne, Lausanne, Switzerland*

[2]*Department of Pathology, Centre Hospitalier Universitaire Vaudois, Ecole Polytechnique Federale de Lausanne, Lausanne, Switzerland*

[3]*Department of Chemistry, Ecole Polytechnique Federale de Lausanne, Lausanne, Switzerland*

Background: The pre-conditioning of tumor vessels by low-dose photodynamic therapy (L-PDT) was shown to enhance the distribution of chemotherapy in different tumor types. However, how light dose affects drug distribution and tumor response is unknown. Here we determined the effect of L-PDT fluence on vascular transport in human mesothelioma xenografts. The best L-PDT conditions regarding drug transport were then combined with Lipoplatin® to determine tumor response.

Methods: Nude mice bearing dorsal skinfold chambers were implanted with H-Meso1 cells. Tumors were treated by Visudyne®-mediated photodynamic therapy with 100 mW/cm^2 fluence rate and a variable fluence (5, 10, 30, and 50 J/cm^2). FITC-Dextran (FITC-D) distribution was assessed in real time in tumor and normal tissues. Tumor response was then determined with best L-PDT conditions combined to Lipoplatin® and compared to controls in luciferase expressing H-Meso1 tumors by size and whole body bioluminescence assessment (n = 7/group).

Results: Tumor uptake of FITC-D following L-PDT was significantly enhanced by 10-fold in the 10 J/cm^2 but not in the 5, 30, and 50 J/cm^2 groups compared to controls. Normal surrounding tissue uptake of FITC-D following L-PDT was significantly enhanced in the 30 J/cm^2 and 50 J/cm^2 groups compared to controls. Altogether, the FITC-D tumor to normal tissue ratio was significantly higher in the 10 J/cm^2 group compared others. Tumor growth was significantly delayed in animals treated by 10 J/cm2-L-PDT combined to Lipoplatin® compared to controls.

Conclusions: Fluence of L-PDT is critical for the optimal distribution and effect of subsequently administered chemotherapy. These findings have an importance for the clinical translation of the vascular L-PDT concept in the clinics.Lasers Surg. Med. 47:323–330, 2015.

Key words: photodynamic therapy; drug/light conditions; tumor response; mesothelioma lipoplatin®

INTRODUCTION

Photodynamic therapy (PDT) consists in the administration of a photosensitizer which, after activation by non-thermal light produces a variety of biological changes in normal and tumor tissues [1]. In cancer, PDT was initially designed to destroy tumor cells [1]. More recently, PDT was also shown to induce a variety of vascular changes ranging from a transient vasospasm, drug convection enhancement in tumor neovessels to a complete tumor vascular shutdown [2–7]. The vascular effect of PDT depends on the photosensitizer type and dose, the drug/light interval, the optical fluence rate, total fluence and the tissue properties (i.e. oxygen supply and levels) [8]. The complex relationship between these parameters for vascular modulation and drug distribution enhancement has been widely studied in normal tissues but is not well known in tumors [8–10]. In addition, the effect of fluence on the tumor and normal tissue vascular transport enhancement is currently a matter of debate [5].

We and others have shown that low-dose vascular photodynamic therapy (L-PDT) could enhance the extravasation of macromolecular compounds into tumors in a variety of tumor types in different rodent models [2,3,5,11–13]. The enhanced drug penetration in tumors was observed with different modes of chemotherapy administration (intravenous and isolated lung

[#]Yabo Wang, Xingyu Wang, Jean Y Perentes, and Thorsten Krueger contributed equally to this work.

Conflict of Interest Disclosures: All authors have completed and submitted the ICMJE form for disclosure of potential conflicts of interest and none were reported

[*]Corresponding authors: Dr Thorsten Krueger and Dr Jean Y Perentes, Service de Chirurgie Thoracique et Vasculaire, Rue du Bugnon 46, 1011 Lausanne, E-mail: Thorsten.Krueger@chuv.ch, Jean.Perentes@chuv.ch

Accepted 30 November 2014
Published online 12 January 2015 in Wiley Online Library (wileyonlinelibrary.com).
DOI 10.1002/lsm.22329

perfusion) and with different types of chemotherapeutics [2,3,5,11,12].

Macromolecular therapeutics (>100 nm in diameter) are known to depend on vascular convection for their extravasation between the intra- and extra-vascular spaces [14]. The latter is depicted by Starling's equation which includes two main parameters: tumor hydrostatic and oncotic pressures. A hallmark of malignant cancer is the high vascular permeability of neovessels associated to increased interstitial fluid pressure (IFP) which hinders convection and drug delivery [15–17]. We have recently shown that L-PDT could cause a transient drop in tumor but not normal tissue IFP while keeping tumor blood flow constant and cause enhanced drug convection in a somewhat similar phenomenon to vascular normalization [4].

While it was shown that PDT administered with a high fluence could cause drug convection enhancement in normal tissue, the optimal fluence conditions for specific tumor drug delivery improvement without affecting normal tissue are currently unknown [4,5,9,10]. Also, although drug distribution enhancement was demonstrated by L-PDT pre-treatment of tumors, it was never demonstrated that this phenomenon corresponded to a better drug efficiency on tumors.

Here, we assessed, by intravital microscopy, the changes induced in tumor and normal tissue vasculature by L-PDT administered with different fluences in a model of H-Meso1 xenograft grown in dorsal skinfold chambers. Based on these results, we defined optimal L-PDT conditions and combined this therapy with the administration of a single dose of liposomal cisplatin (Lipoplatin®). Using H-Meso1 tumors transfected with a luciferase construct, we determined the changes in tumor cell viability and size in animals treated with combined therapy (L-PDT + Lipoplatin®) compared to controls (L-PDT alone, Lipoplatin® alone and controls) over a period of 28 days.

MATERIAL AND METHODS

Animal Model

Dorsal skinfold chamber. A human mesothelioma tumor cell line (H-Meso1, Mason Worcester, MA, USA) was implanted for donor tumor generation by injecting a 0.1 ml cell suspension containing 2×10^7 tumor cells behind the left scapula of nude mice (Charles River, France). Tumors were grown up to 8 mm in diameter. The donor animals were then sacrificed and the tumors were cut into chunks that were used for dorsal skinfold chamber implantation. A custom built dorsal skinfold chamber was implanted on the back of nude mice (Charles River, France). This window was a custom design that has the advantage to only weight 2 g and allow full tumor and surrounding tissue observation thanks to the big size coverslip. The model builds on a previously described one from our laboratory [10]. Tumor chunks were prepared by removing the capsule and the necrotic portions of the donor tumor and by cutting the remaining tumor in $2 \times 2 \times 2$ mm cubes which were placed in a Petri dish and immersed with cold PBS. The pieces were then placed into the center of the dorsal skinfold chambers. The vascularization of the implanted tumor chunks was checked daily and the experiments began when a stable perfused vasculature was visible using transillumination microscopy (in general after 14 days). Tumor size at that time was of approximately 4×4mm

Subcutaneous implantation of H-Meso1-Luc. To evaluate the effect of combined L-PDT therapy at the optimal fluence in combination with chemotherapy on tumor growth, we used a heterotopic model of mesothelioma transfected with luciferase (H-Meso1-Luc). Animals were implanted with H-Meso1-Luc cells by injecting a 0.1 ml cell suspension containing 2×10^7 tumor cells behind the left scapula. The intra-peritoneal injection of luciferin is degraded by the luciferase and creates light that can be measured by a bioluminescence assay (see methods on whole body imaging). When tumors reached 30mm3, animals were randomly assigned to either control, L-PDT alone, Lipoplatin™ alone or L-PDT combined to Lipoplatin™. Luciferin was injected at 75 mg/kg. After 10 minutes and for 30 minutes, whole body bioluminescence was performed. All animals were kept in a sterile environment and the experiments were conducted in accordance with the National law and Institutional guidelines for animal care and use.

Photodynamic Therapy

Animals included in the study underwent, according to treatment groups, low-dose photodynamic therapy. For this, Visudyne®, the photosensitizer, was administered intravenously at a concentration of 400 ug/kg. After a drug/light interval of 10 minutes, light was administered at a fluence rate of 100 mW/cm^2 for a total fluence of 5, 10, 30 and 50 J/cm^2. This was performed using a 690 nm laser coupled to a 600um fiber containing a frontal light distributor with a lens (Medlight, Ecublens, Switzerland). Laser power and light dose were calculated based on the geometry of the light path in order to irradiate the entire window or tumor (tumor + normal tissue) with a total light dose of 5–10–30 and 50J/cm^2. These doses were chosen based on previously published experiments.

Intravital Microscopy

To evaluate the role of L-PDT fluence variation (5, 10, 30, and 50 J/cm2) on the vascular transport of tumor/normal tissues (FITC-Dextran 2MDa distribution, FITC-D) we used nude mice bearing dorsal skinfold chambers and implanted with H-Meso1 tumors. Tumors were treated with L-PDT and had FITC-D injection after 60 minutes. The distribution of FITC-D was assessed over a period of 45 minutes by epifluorescence microscopy. For this, a Carl Zeiss Axiotech Vario 100 microscope was used for in vivo observation of the dorsal skinfold chamber. For that purpose, the mouse was placed in a lateral decubitus position inside a plexiglas tube that was positioned under the microscope. The chamber on the back of the mouse was fixed horizontally such that its position under the

microscope allowed trans-illumination and at the same time epi-illumination for fluorescence microscopy. Animals were anesthetized by ketamine (80 mg/kg) and xylazine (10 mg/kg). Achroplan Carl Zeiss 4x/0.10 Plan Neofluar objectives were used for a large field of view (3×3 mm). Fluorescence excitation was performed via a filtered 100 W HBO103 light source (OSRAM GmbH, Augsburg, Germany), powered through a variable Carl Zeiss FluoArc device. A Uniblitz shutter VS25 with its controller VMM-D1 (Vincent Associates, Rochester, NY, USA) was used to cut off the light from the HBO lamp. Images and video sequences were recorded with an on chip amplified electron multiplier consisting of a back illuminated thinned Peltier cooled CCD camera (EM-CCD C9100–12,400 to 1000 nm, Hamamatsu Photonics, Solothurn, Switzerland) allowing for an up to 2000x amplified signal gain. This set-up allowed the excitation light to be lowered, so as to prevent both PDT and photobleaching from the analysis light. Images and sequences were recorded through the Hamamatsu camera controller with the Hamamatsu HiPic version 7.0 software, producing 16 bit grey level images with a size of 512×512 pixels. A Multiscan Rate Converter MSC-12A-HPK (Stack Ltd, Saitama, Japan) was added between the EM-CCD and the controller providing digital and video signals in parallel.

Quantification of FITC Dextran Leakage in Tumor and Normal Tissues

The extravasations of FITC-D was determined by epifluorescence microscopy, using excitation light from a Hg-arc lamp filtered at 470 ± 20 nm by a Carl Zeiss "cube filter set 09" (Exc. BP 450–490, DMFT510, Em. LP515) with the 4x objective. The daily stability of the Hg-arc lamp was tested using a rubis 8Sp3 disc (diameter 12 mm, thickness 1 mm, Hans Stettler, Lyss, Switzerland) as previously described [9]. FITC-D fluorescence was recorded in regions of entire dorsal skinfold chamber consisting of tumor and normal tissue with different treatment schemes. The intensity values of FITC-D were recorded before, and every 10 minutes following intravenous injection. All intensity values for each observed region were normalized to their initial value for analysis by using a public domain ImageJ (version 1.37) software (Rasband, W.S., ImageJ, US National Institute of Health, Bethesda, Maryland, USA). This measurement was performed in the tumor and in the normal surrounding tissue. Quantification was performed in 5 animals per group and analyzed as described in the statistical analysis section.

Cell Culture and Luciferase Transfection

The human mesothelioma cell line H-Meso-1 was transfected using a luciferase lentiviral construct (pGL3). The latter was a kind gift from the Naldini Lab. The resulting plasmid was sequenced to verify the presence and integrity of the inserted luciferase cDNA. Parental human mesothelioma cells (H-Meso1) were cultured in DMEM supplemented with 10% FBS in a humidified 5% CO_2 incubator at 37 °C. Bulk cells transduced with luciferase were obtained after two rounds of lentiviral infection for 8 hours and selected for puromycine selection. The efficiency of luciferase expression was then assessed in vitro by adding luciferin in the culture medium at 150 ug/ml and checking for light emission with the bioluminescence assay.

In Vivo Bioluminescence Imaging

Tumor sizes were evaluated via in vivo bioluminescence using the IVIS Imaging 200 series system (Xenogen Caliper Life Sciences, Hopkinton Massachusetts, USA). For this, animals were injected with luciferin intraperitoneally (75mg/kg). After 10 minutes, bioluminescence signals were captured sequentially over 30 min. Maximal photon flux images were acquired in the region of the interest using Living Image Software (Xenogen) to generate the tumor growth curve. Data were expressed as photon emission density (photons/s/cm^2).

Tumor Size Assessment

Tumors were measured on daily basis using a caliper. The volume of each tumor was calculated by length times width to the power of 2 and divided by 2.

Statistical Analysis

A paired student's two-tailed t-test was used to calculate statistical differences of fluorescence ratios between the 5 and 50 minutes time-points in the same groups. To analyze the variables "fluorescence ratio" at a 50 minutes time-point in all groups, we applied an ANOVA test with Tukey's HDS post hoc test for multiple comparisons. Bioluminescence data for the tumor growth curve were compared between groups using an ANOVA test. Data were expressed as Mean $\pm$ standard deviation. Graphs and statistics were obtained using GraphPad Prism 5.0 (GrphPad Software, Inc., California, USA) and STAT software (version 12.1, StataCorp LP, College Station, Texas, USA). A P-value < 0.05 was considered as significant.

RESULTS

Light Dose During Low-Dose PDT is Critical for Selective Tumor Drug Uptake Enhancement

In a first set of experiments, we treated H-Meso1 tumors grown in dorsal skinfold chambers by L-PDT using a fluence of 5, 10, 30, and 50 J/cm2 (Fig. 1A). Animals underwent epifluorescence intravital microscopy following FITC-D injection. This allowed FITC-D distribution assessment over a period of 45 minutes. Typical images of the intravital imaging of FITC-D over time are shown for the different treatment groups (Fig. 1B). We observed that 30 and 50J/cm^2 treatments caused clear occlusion of the tumor vasculature while normal tissue demonstrated enhanced drug uptake (Fig. 1A). FITC-D leakage in the different tissue compartments (tumor/normal) were quantified over time (Fig. 2A). We found that FITC-D leakage in tumors was significantly enhanced in the 10 J/cm^2 group

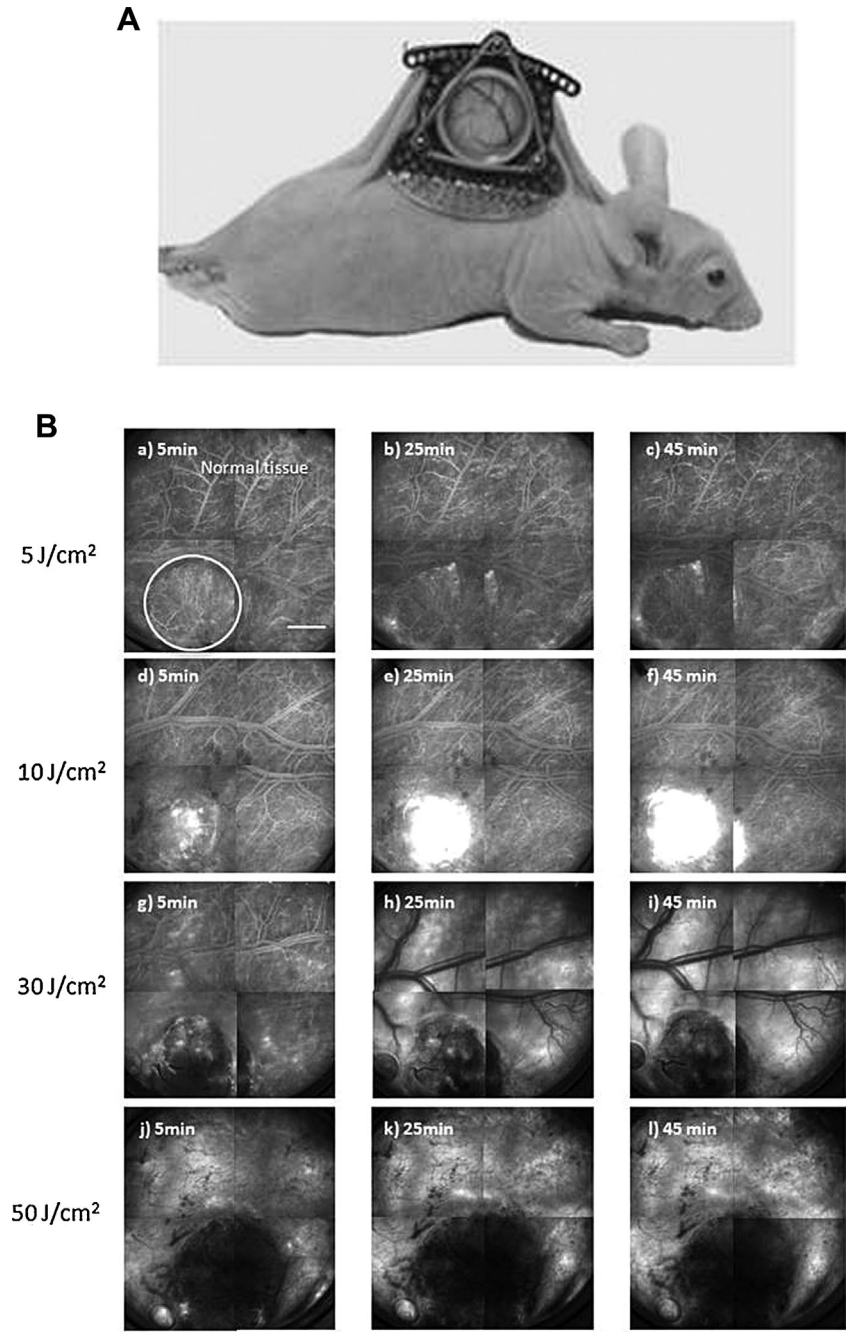

Fig. 1. **a**), Nude mouse bearing a custom designed dorsal skinfold chamber. This window model has the advantage to be very light compared to other systems available (2 g in weight) and to enable full tumor observation because of the big window coverslip; **b**), intravital epifluorescent imaging of the distribution of FITC-D in the tumor and normal tissue of H-Meso1 tumors grown in dorsal skinfold chambers. Three sequences (a-c, d-f, g-h and h-j) per treatment group (fluence of 5, 10, 30, and 50 J/cm^2) are represented for time points 5, 25, and 45 minutes following FITC-D injection. FITC-D leakage distributed in normal and tumor tissue after 5 J/cm^2 but the accumulation of FITC-D in tumors was increased with 10 J/cm^2. Higher L-PDT fluence (30 and 50 J/cm^2) caused a vascular shutdown of the tumor vasculature while normal tissue leakage was enhanced.

compared to the 5 J/cm^2 group (Fig. 2A). Interestingly, the FITC-D quantification in tumors in the 30 and 50 J/cm2 groups showed enhanced uptake. However, a precise analysis of the tumor vasculature showed clear tumor vascular shutdown and the FITC-D intensity increase was due to enhanced leakage of the FITC-D in normal tissue located behind the observed tumor. Regarding normal tissue FITC-D uptake, no change in normal tissue uptake was observed between 5 and 10 J/cm^2 treatments while 30 and 50 J/cm^2 treatments caused significant FITC-D distribution enhancement. We then plotted tumor to normal tissue FITC-D uptake ratio to assess the best light dose range for maximal FITC-D uptake in tumors with minimal change in normal tissue (Fig. 2C). We found that 10 J/cm^2 was the optimal L-PDT light dose for best distribution in tumors with minimal normal tissue leakage.

Effect of Low-Dose PDT Combined With Systemic Lipoplatin® Chemotherapy on Tumor Response

To determine if the enhanced distribution in chemotherapy induced by L-PDT translated into a better tumor response, we determined the growth of subcutaneous tumors that express luciferase using calliper measurements and whole body bioluminescence assay (Fig. 3A, B). Luciferin was injected intra-peritoneally and, in viable tumor cells that expressed luciferase, caused the creation of light that could be quantified by bioluminescence. This model allowed a precise quantification of the viable tumor cells by whole body luminescence imaging. We treated animals by L-PDT alone (10J /cm2), Lipoplatin™ alone, L-PDT + Lipoplatin™ and no treatment. Tumor viability was then assessed using the bioluminescence assay. We found that L-PDT alone and Lipoplatin™ alone caused a

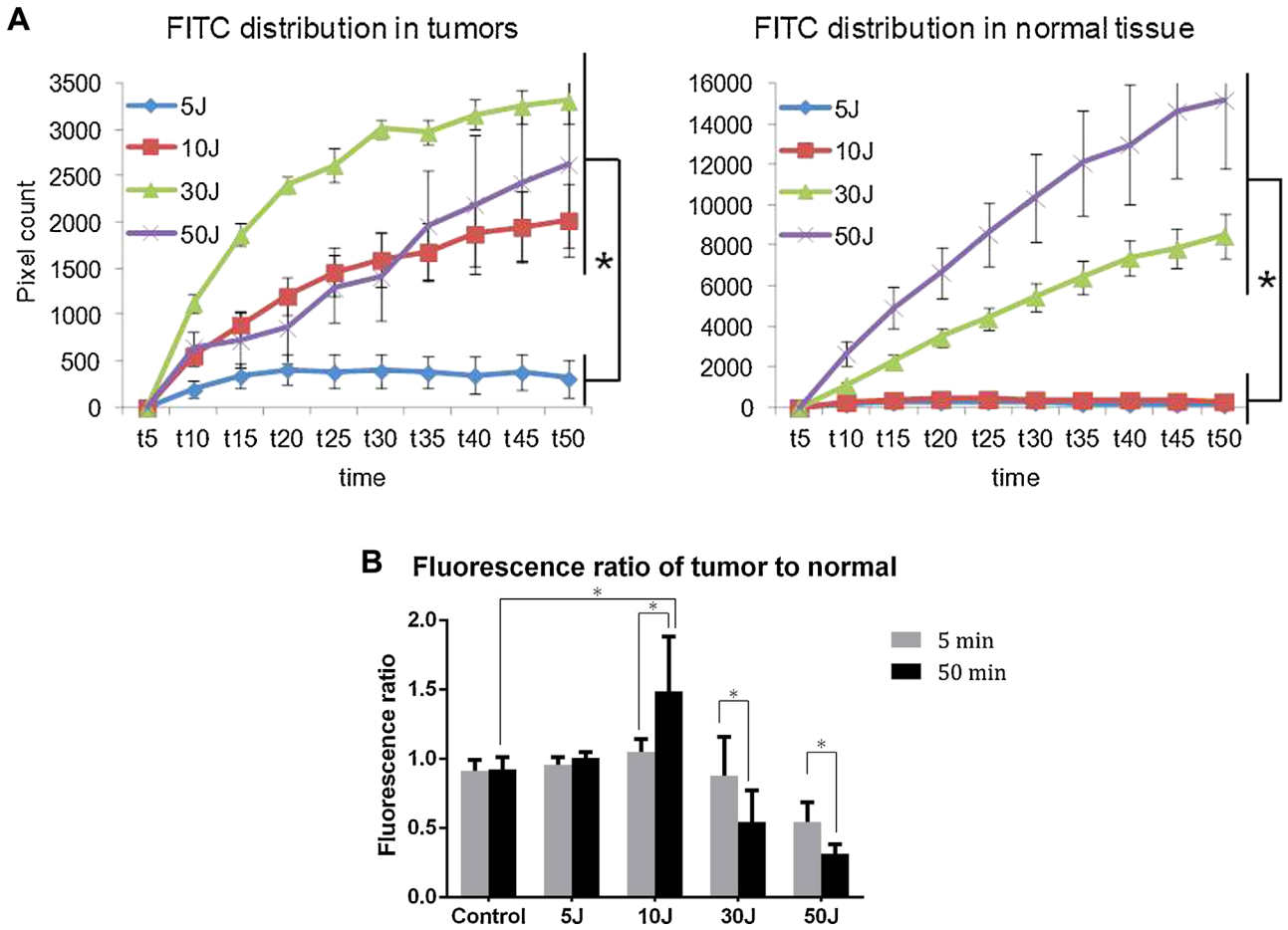

Fig. 2. **a**), FITC-D fluorescence quantification in tumor and normal tissues over time (50 minutes) after low-dose PDT with different irradiances (5 animals/group). FITC-D fluorescence accumulation in tumors was significantly enhanced with 10 J/cm2 compared to 5 J/cm2 conditions. For higher doses of irradiance (30 and 50 J/cm2), FITC-D did not circulate in tumor vessels (that were clogged) but fluorescence in the normal tissue was enhanced significantly. Overall, 10J/cm2 irradiance had the best effect on tumor uptake of FITC-D with no effect in the normal tissue. **b**), Tumor to normal FITC-D fluorescence plotted at 5 and 50 minutes following FITC-D injection for different L-PDT conditions or control (Visudyn with no light administration). L-PDT at a 10 J/cm^2 fluence caused a significantly better tumor to normal tissue uptake of FITC-D than all other PDT conditions and therefore appears to be the most favorable for FITC-D distribution in tumors while limiting normal tissue uptake (*: $P < 0.05$).

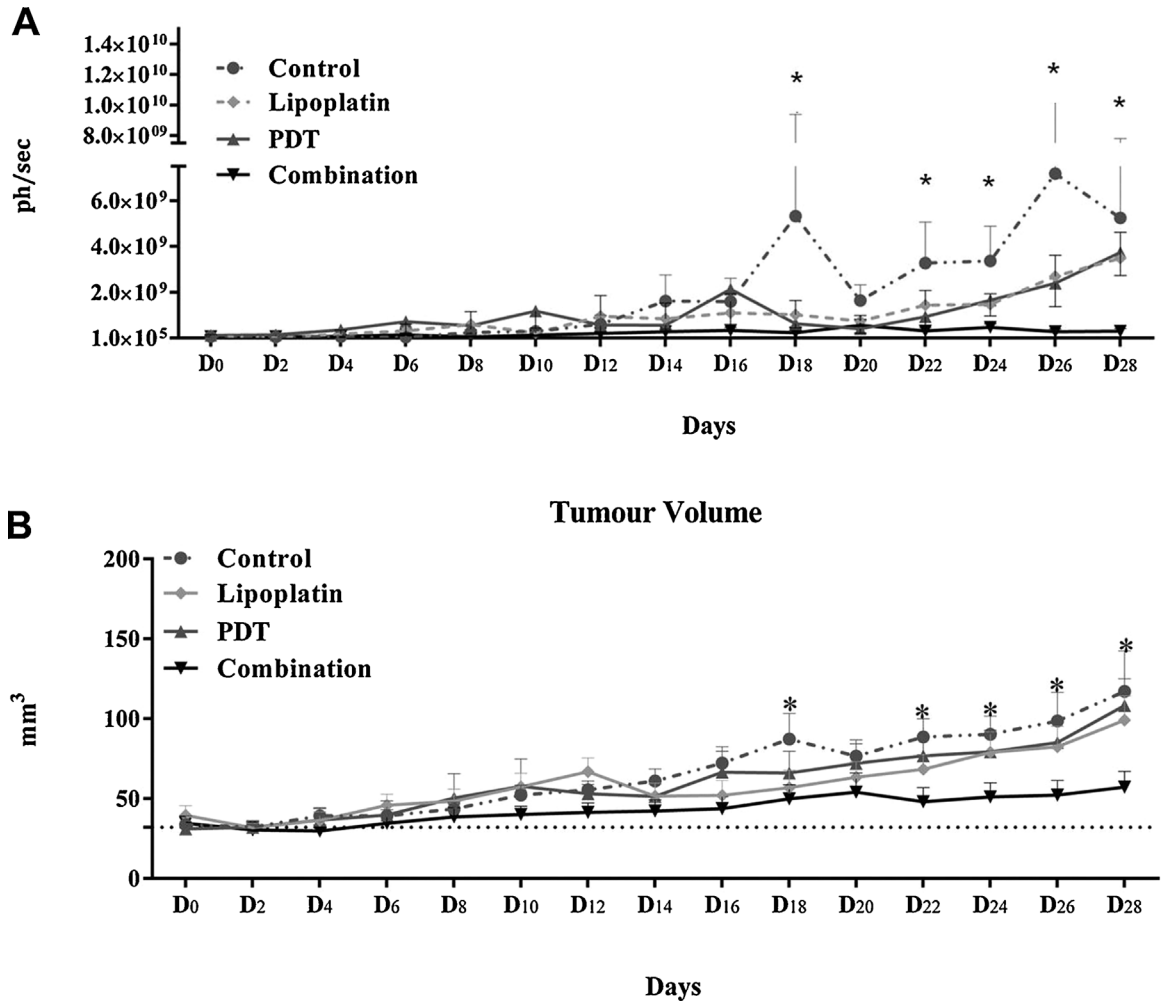

Fig. 3. **a**) Bioluminescence assay quantification of the growth of H-Meso1-luc tumors over a period of 28 days treated either by L-PDT 10 J/cm^2 alone, Lipoplatin® alone, L-PDT 10 J/cm^2 + Lipoplatin® and untreated controls. Tumor growth curves showed a significant tumor growth delay after combined treatment compared to controls (*: $P < 0.05$ of control photoluminescence values compared to combination treatment). **b**) Tumor growth curves of control, Lipoplatin® alone, L-PDT 10 J/cm2 alone and combined treatment are shown over time. Combined therapy shows significantly lower sizes of tumors compared to the control tumors (*: $P < 0.05$).

slight decrease in tumor growth compared to controls although not significant (Fig. 3A). However, combination therapy caused a persistant and long lasting drop in tumor growth that was significant and that lasted up to 28 days. These findings were also found with calliper measurements of the tumor volume that was significantly lower over time in the combined treatment compared to control (Fig. 3B).

DISCUSSION

In the current study, we evaluated the efficacy and selectivity of Visudyne® -mediated low-dose PDT at different fluences in an H-Meso1 heterotopic xenograft model in nude mice. In this model, we found that a fluence of 10 J/cm^2 with a fluence rate of 100 mW/cm^2 were optimal to enhance vascular transport of macromolecules in tumors while leaving normal tissues unaffected. It was previously shown that L-PDT could enhance the distribution of chemotherapeutics in various tumor models including colon cancer, mesothelioma, adenocarcinoma, prostate cancer and sarcoma [2,3,5,9–13]. Most of these studies used different photosensitisers with fluence rates ranging between 3 and 100mW/cm^2 and fluences ranging between 10 and 88J/cm^2. The importance of fluence and fluence rates were studied in a model of colon cancer [5]. It was shown that vascular L-PDT enhanced tumor drug distribution when fluence ranged between 48 and 88 J/cm^2 with fluence rates ranging between 14 and 28 mW/cm^2 [5]. Interestingly, the study did not look at higher fluence rates because of light exposure timing issues making these

conditions difficult to compare to what was reported. Fluence and fluence rates are of major importance as they affect the photodynamic reaction, creation of oxygen species and oxygen depletion which are key for the biological effects of PDT [8]. In addition, vascular modulation by photodynamic therapy also involves the optimal location of the photosensitizer in the perivascular area (typically estimated at 15 minutes after photosensitizer injection for Visudyne®). In this study, we chose an alternative approach to the previously published studies and used a high fluence rate of 100 mW/cm^2 with low fluencies ranging between 5 and 50 J/cm^2. The major rational for a high fluence rate was to have a rapid light delivery and take maximal advantage of the short perivascular location of Visudyne® for best vessel modulation. In addition, based on previous data published by our group and others, we chose a fluence range that covered tumor and normal tissue vessel modulation. Our findings are concordant with previously published data with the advantage our light distribution was shorter. This approach did not preclude vascular modulation by L-PDT [5,8].

In our study, we found that L-PDT fluence variation had different effects in normal and tumor tissues. For tumors, our findings show there was an optimal fluence for maximal vascular transport enhancement. Any variation from the optimal fluence (lower or higher fluencies) caused either no vascular enhancement or tumor vascular shutdown. In normal tissue however, increasing fluencies enhanced vascular transport in a somewhat linear fashion. Previous observations have already suggested that the mechanism for drug distribution enhancement by L-PDT is different in normal and tumor tissues [4]. In normal tissues, it was demonstrated that the fluencies required for drug distribution enhancement are, on average, 10 fold higher to the ones necessary in tumor tissues [9,10,13]. Also, although the precise mechanism for vascular transport enhancement is not well known, it was demonstrated that selectins and the immune system played an important role for drug distribution enhancement in normal tissue while this was not the case in tumor tissues [9,10]. Here, we were able to show that the different effects of L-PDT between normal and tumor tissues can be exploited: with a fluence of 10 J/cm^2, we were able to significantly enhance drug distribution in tumors while leaving normal tissues unaffected. In addition, this study shows the value of the differential L-PDT effect between normal and tumor tissues which can be exploited to selectively target cancer while avoiding excessive normal tissue accumulation and toxicity.

A clinical translation of our study in patients, although the procedure remains complex and invasive, could be of interest in superficially spreading tumors such as mesothelioma or oligometastatic pleural disseminations. Indeed, this therapy has limited side effects while enhancing drug distribution in tumors significantly. However optimal drug/light conditions are mandatory for tumor blood vessel L-PDT to be successful. Therefore, a better understanding of how photosensitization modifies the vascular function and refinements of *in situ* L-PDT monitoring are mandatory for the translation of this concept in a clinical setting. Few parameters currently exist to assess the impact of L-PDT on the vasculature and thus determine the appropriate sequence of administration of chemotherapy following L-PDT for best therapeutic results. Based on our findings, the choice of the fluence should be sufficiently high to enhance drug distribution in tumors but low enough not to affect normal tissue and cause morbidity. In addition to the fluence and fluence rate monitoring, one approach could consist in the assessment of interstitial fluid pressure and laser Doppler blood flow in tumor and normal tissues which were shown to well correlate with the drug distribution enhancement effect of L-PDT [4].

In this study, we have observed, in real time, the vascular transport changes of living tumors and surrounding normal tissue following L-PDT. Intravital microscopy is a complex but robust methodology to visualize the result of a therapy on the tumor and its environment [17–20]. The time lapse experiments using the optimal 10 J/cm^2 fluence showed that L-PDT caused enhanced vascular transport in tumors but not normal tissues. The macromolecular dye FITC-D was chosen in this study as its size is comparable to modern macromolecular cytostatic compounds (100 nm). Due to its fluorescent properties, we could document by intravital fluorescence microscopy its intravascular distribution after intravenous injection. FITC-D was injected one hour after L-PDT as previous work has suggested that vascular convection was enhanced during the first hour following L-PDT [5]. We found that FITC-D kept accumulating in tumor tissue but not normal tissue with the optimal L-PDT light fluence and reached a plateau approximately 45 minutes after injection (1 h45 after L-PDT treatment). These findings suggest that the vascular changes in tumors induced by L-PDT are long-lasting and suggest a change in the vascular structure rather than a vasospasm. This is of interest as it could be exploited for repeated chemotherapy administration regimens according to the duration of the enhanced drug distribution window induced by L-PDT. Previous work has shown that a single PDT treatment could cause sequential vascular changes that were durable over time [1,21] but further studies are required to better define the vascular enhancement window. Altogether, our data show the robustness of our animal model for multiple timepoint vascular modulation observations with each timepoint being compared to the initial situation. From a statistical perspective, the quality of our data was enhanced by this approach.

Finally, we determined tumor response following L-PDT combined to Lipoplatin®. For this, we chose a macromolecular liposomal form of cisplatin, a drug currently used for the treatment of malignant pleural mesothelioma. The liposomal formulation of cisplatin was developed to reduce its systemic toxicity while simultaneously improving its efficacy [22,23]. The ideal L-PDT treatment conditions (10 J/cm^2) were selected according to the first part of the study in order to achieve selective tumor drug delivery. We observed a strong and significant effect on tumor growth of L- PDT combined to systemic chemotherapy, compared to

control animals (no treatment or L-PDT/Lipoplatin® alone). The combined L-PDT + Lipoplatin® group had a long lasting tumor growth decrease with no clear evidence of tumor regrowth at 28 days. When comparing this to the L-PDT and Lipoplatin® monotherapy, the combined treatment group seemed to be synergistic. Further work is required to prove this element. However, this finding is of major importance for the L-PDT concept validation in the clinics.

We conclude that photodynamic drug delivery with the appropriate fluence and fluence rate has the potential to increase tumor uptake of systemically administrated drugs in a tumor-specific fashion.

REFERENCES

1. Dolmans DE, Fukumura D, Jain RK. Photodynamic therapy for cancer. Nat Rev Cancer 2003;3(5):380–387. doi: 10.1038/nrc1071.
2. Chen B, Crane C, He C, Gondek D, Agharkar P, Savellano MD, Pogue BW. Disparity between prostate tumor interior versus peripheral vasculature in response to verteporfin-mediated vascular-targeting therapy. Int J Cancer 2008;123-(3):695–701. doi: 10.1002/ijc.23538.
3. Chen B, Pogue BW, Zhou X, O'Hara JA, Solban N, Demidenko E, Hasan T. Effect of tumor host microenvironment on photodynamic therapy in a rat prostate tumor model. Clin Cancer Res 2005;11(2 Pt 1): 720–727.
4. Perentes, JY, Wang Y, Wang X, Abdelnour E, Gonzalez M, Decosterd L, Krueger T. Low-dose vascular photodynamic therapy decreases tumor interstitial fluid pressure, which promotes liposomal doxorubicin distribution in a murine sarcoma metastasis model. Transl Oncol 2014;7(3):393–399. doi: 10.1016/j.tranon.2014.04.010.
5. Snyder JW, Greco WR, Bellnier DA, Vaughan L, Henderson BW. Photodynamic therapy: A means to enhanced drug delivery to tumors. Cancer Res 2003;63(23):8126–8131.
6. Wang Y, Gonzalez M, Cheng C, Haouala A, Krueger T, Peters S, Debefve E. Photodynamic induced uptake of liposomal doxorubicin to rat lung tumors parallels tumor vascular density. Lasers Surg Med 2012;44(4):318–324.
7. Wang Y, et al. Photodynamic drug delivery enhancement in tumours does not depend on leukocyte-endothelial interaction in a human mesothelioma xenograft model. Eur J Cardiothorac Surg 2012;42(2):348–354.
8. Henderson BW, Gollnick SO, Snyder JW, Busch TM, Kousis PC, Cheney RT, Morgan J. Choice of oxygen-conserving treatment regimen determines the inflammatory response and outcome of photodynamic therapy of tumors. Cancer Res 2004;64(6):2120–2126.
9. Debefve E, Cheng C, Schaefer SC, Yan H, Ballini JP, van den Bergh H, Krueger T. Photodynamic therapy induces selective extravasation of macromolecules: Insights using intravital microscopy. J Photochem Photobiol B 2010;98(1):69–76. doi: 10.1016/j.jphotobiol.2009.11.006.
10. Debefve E, Mithieux F, Perentes JY, Wang Y, Cheng C, Schaefer SC, Krueger T. Leukocyte-endothelial cell interaction is necessary for photodynamic therapy induced vascular permeabilization. Lasers Surg Med 2011;43(7):696–704. doi: 10.1002/lsm.21115.
11. Cheng C, Debefve E, Haouala A, Andrejevic-Blant S, Krueger T, Ballini JP, Ris HB. Photodynamic therapy selectively enhances liposomal doxorubicin uptake in sarcoma tumors to rodent lungs. Lasers Surg Med 2010;42(5):391–399. doi: 10.1002/lsm.20912.
12. Cheng C, Haouala A, Krueger T, Mithieux F, Perentes JY, Peters S, Ris HB. Drug uptake in a rodent sarcoma model after intravenous injection or isolated lung perfusion of free/liposomal doxorubicin. Interact Cardiovasc Thorac Surg 2009;8(6):635–638. doi: 10.1510/icvts.2008.194720
13. Cheng C, Wang Y, Haouala A, Debefve E, Andrejevic Blant S, Krueger T, Perentes JY. Photodynamic therapy enhances liposomal doxorubicin distribution in tumors during isolated perfusion of rodent lungs. Eur Surg Res 2011;47(4):196–204. doi: 10.1159/000330744.
14. Chauhan VP, Stylianopoulos T, Martin JD, Popovic Z, Chen O, Kamoun WS, Jain RK. Normalization of tumour blood vessels improves the delivery of nanomedicines in a size-dependent manner. Nat Nanotechnol 2012;7(6):383–388. doi: 10.1038/nnano.2012.45.
15. Jain RK. Therapeutic implications of tumor physiology. Curr Opin Oncol 1991;3(6):1105–1108.
16. Jain RK. The Eugene M. Landis Award Lecture Delivery of molecular and cellular medicine to solid tumors. Microcirculation 1996;4(1):1–23.
17. Tong RT, Boucher Y, Kozin SV, Winkler F, Hicklin DJ, Jain RK. Vascular normalization by vascular endothelial growth factor receptor 2 blockade induces a pressure gradient across the vasculature and improves drug penetration in tumors. Cancer Res 2004;64(11):3731–3736. doi: 10.1158/0008-5472.CAN-04-0074.
18. Jain RK. Normalization of tumor vasculature: An emerging concept in antiangiogenic therapy. Science 2005;307-(5706):58–62. doi: 10.1126/science.1104819.
19. Leunig M, Goetz AE, Gamarra F, Zetterer G, Messmer K, Jain RK. Photodynamic therapy-induced alterations in interstitial fluid pressure, volume and water content of an amelanotic melanoma in the hamster. Br J Cancer 1994;69(1):101–103.
20. Winkler F, et al. Kinetics of vascular normalization by VEGFR2 blockade governs brain tumor response to radiation: Role of oxygenation, angiopoietin-1, and matrix metalloproteinases. Cancer Cell, 2004;6(6):553–563.
21. Dolmans DE, Kadambi A, Hill JS, Flores KR, Gerber JN, Walker JP, Fukumura D. Targeting tumor vasculature and cancer cells in orthotopic breast tumor by fractionated photosensitizer dosing photodynamic therapy. Cancer Res 2002;62(15):4289–4294.
22. Boulikas T. Low toxicity and anticancer activity of a novel liposomal cisplatin (Lipoplatin) in mouse xenografts. Oncol Rep 2004;12(1):3–12.
23. Stathopoulos GP, Boulikas T, Vougiouka M, Rigatos SK, Stathopoulos JG. Liposomal cisplatin combined with gemcitabine in pretreated advanced pancreatic cancer patients: A phase I-II study. Oncol Rep 2006;15(5):1201–1204.

Treatment of Pleural Malignancies by Photo-Induction Combined to Systemic Chemotherapy: Proof of Concept on Rodent Lung Tumors and Feasibility Study on Porcine Chest Cavities

Xingyu Wang,[1] Fabrizio Gronchi,[2] Michael Bensimon,[3] Thomas Mercier,[4] Laurent Arthur Decosterd,[4] Georges Wagnières,[3] Elodie Debefve,[1] Hans-Beat Ris,[1]* Igor Letovanec,[5] Solange Peters,[6] and Jean Yannis Perentes[1]

[1]*Departement of Thoracic Surgery, Centre Hospitalier Universitaire Vaudois, Lausanne, VD, Switzerland*
[2]*Department of Anesthesiology, Centre Hospitalier Universitaire Vaudois, Lausanne, VD, Switzerland*
[3]*Central Environmental Laboratory, Swiss Federal Institute of Technology(EPFL), Lausanne, VD, Switzerland*
[4]*Departement of Pharmacology, Centre Hospitalier Universitaire Vaudois, Lausanne, VD, Switzerland*
[5]*Department of Pathology, University of Lausanne, Lausanne, VD, Switzerland*
[6]*Departement of Oncology, Centre Hospitalier Universitaire Vaudois, Lausanne, VD, Switzerland*

Background: Low-dose, Visudyne®-mediated photodynamic therapy (photo-induction) was shown to selectively enhance tumor vessel transport causing increased uptake of systemically administered chemotherapy in various tumor types grown on rodent lungs. The present experiments explore the efficacy of photo-induced vessel modulation combined to intravenous (IV) liposomal cisplatin (Lipoplatin®) on rodent lung tumors and the feasibility/toxicity of this approach in porcine chest cavities.

Material and Methods: Three groups of Fischer rats underwent orthotopic sarcoma ($n = 14$), mesothelioma ($n = 14$), or adenocarcinoma ($n = 12$) implantation on the left lung. Half of the animals of each group had photo-induction (0.0625 mg/kg Visudyne®, 10 J/cm^2) followed by IV administration of Lipoplatin® (5 mg/kg) and the other half received Lipoplatin® without photo-induction. Then, two groups of minipigs underwent intrapleural thoracoscopic (VATS) photo-induction (0.0625 mg/kg Visudyne®; 30 J/cm^2 hilum; 10 J/cm^2 apex/diaphragm) with *in situ* light dosimetry in combination with IV Lipoplatin® administration (5 mg/kg). Protocol I ($n = 6$) received Lipoplatin® immediately after light delivery and Protocol II ($n = 9$) 90 minutes before light delivery. Three additional animals received Lipoplatin® and VATS pleural biopsies but no photo-induction (controls). Lipoplatin® concentrations were analyzed in blood and tissues before and at regular intervals after photo-induction using inductively coupled plasma mass spectrometry.

Results: Photo-induction selectively increased Lipoplatin® uptake in all orthotopic tumors. It significantly increased the ratio of tumor to lung Lipoplatin® concentration in sarcoma ($P = 0.0008$) and adenocarcinoma ($P = 0.01$) but not in mesothelioma, compared to IV drug application alone. In minipigs, intrapleural photo-induction combined to systemic Lipoplatin® was well tolerated with no toxicity at 7 days for both treatment protocols. The pleural Lipoplatin® concentrations were not significantly different at 10 and 30 J/cm^2 locations but they were significantly higher in protocol I compared to II (2.37 ± 0.7 vs. 1.37 ± 0.7 ng/mg, $P < 0.001$).

Conclusion: Visudyne®-mediated photo-induction selectively enhances the uptake of IV administered Lipoplatin® in rodent lung tumors. Intrapleural VATS photo-induction with identical treatment conditions combined to IV Lipoplatin chemotherapy is feasible and well tolerated in a porcine model. Lasers Surg. Med.

Key words: adenocarcinoma; mesothelioma; sarcoma; rodent; minipig; lung; lipoplatin; chemotherapy; photodynamic therapy; visudyne

INTRODUCTION

Malignant pleural disease is a frequently observed clinical entity that has an important social, medical, and economic burden [1]. Current treatment is based on systemic cisplatin-based chemotherapy but success is limited due, in part, to the poor penetration of cytostatic agents into tumors. Recently, several studies have shown

Conflict of Interest Disclosures: All authors have completed and submitted the ICMJE Form for Disclosure of Potential Conflicts of Interest and none were reported.

Xingyu Wang, Fabrizio Gronchi, Solange Peters, and Jean Yannis Perentes contributed to this work equally.

Contract grant sponsor: Swiss National Foundation; Contract grant numbers: 3200030, 135197.

*Correspondance to: Hans-Beat Ris, MD, Service de chirurgie thoracique, CHUV, rue du Bugnon 21, 1011 Lausanne. E-mail: hans-beat.ris@chuv.ch

Accepted 13 September 2015
Published online in Wiley Online Library (wileyonlinelibrary.com).
DOI 10.1002/lsm.22422

that vessel targeted photodynamic therapy (PDT) at low drug-light conditions could selectively enhance the uptake and distribution of subsequent systemically administered macromolecular cytostatics in tumors. Interestingly, this pre-treatment step had no effect on the surrounding normal tissue which suggested vessel targeted low-dose PDT had a tumor specific effect (photo-induction) [2–6]. We and others have shown that Visudyne®-mediated photo-induction selectively increased the uptake of liposomal cytostatics to pleural tumors grown orthotopically in rodents[3–5] and delayed tumor growth of human mesothelioma xenografts compared to chemotherapy alone [6]. It is therefore, suggested that intrapleural photo-induction may enhance the uptake of subsequently applied cytostatics such as macromolecular cisplatin to selectively enter pleural tumors and thereby improve treatment outcome.

Recently, liposomal cisplatin (Lipoplatin®) has been formulated and tested thoroughly in preclinical and phase I, II, and III trials for various malignancies. It is expected to be applied in pleural malignancies in the near future [7–9]. Therefore, in the present preclinical study, we investigate the effect of intrapleural Visudyne®-mediated photo-induction combined to systemic Lipoplatin® chemotherapy on various subpleural tumor types grown orthotopically on rodent lungs (proof of concept) and then assess the feasibility and toxicity of this approach applied by video-assisted thoracoscopic surgery (VATS) in the pleural cavities of minipigs.

MATERIALS AND METHODS

Photo-Induction and Systemic Lipoplatin® Chemotherapy on Tumors Grown

Study design. Three groups of Fischer rats underwent orthotopic subpleural generation of sarcoma ($n = 14$), mesothelioma ($n = 14$), or adenocarcinoma ($n = 12$) in the lower lobe of the left lung. When the tumors had reached a size of 4–6 mm in diameter, half of the animals of each group underwent low-dose Visudyne®-mediated photodynamic therapy (photo-induction) of the tumor and the surrounding lower lobe followed immediately after light delivery by intravenous (IV) injection of Lipoplatin® that was allowed to circulate for 60 minutes. At this time point, the treated tumor and surrounding lung were harvested and processed for Lipoplatin® tissue concentration measurements. The other half of the animals of each group underwent Lipoplatin® administration without photo-induction (controls).

Animals and housing. Forty male Fischer rats (Charles River, France) weighting 250–300 g were used and treated in accordance with the National Institute of Health Guidelines for the Care and Use of Laboratory Animals and the Local Ethical Committee of the University of Lausanne.

Tumor cell lines. Syngeneic mesothelioma II-45 and methylcholanthrene-induced sarcoma cell lines were cultivated at 37°C with 5% CO_2 in 20 ml of RPMI-1,640 medium containing glutaril, 10% fetal bovine serum (FBS), and 1% penicillin/streptomycin (Invitrogen Corporation, GIBCOTM Life Technologies Ltd, Paisley, UK). A syngeneic adenocarcinoma cell line (13,762 MAT B III) was cultivated at 37°C with 5% CO_2 in 20 ml of McCoy's 5a medium containing 1.5 ml L-Glutamin and 2.2 g/L sodium bicarbonate, 10% FBS (Invitrogen Corporation, GIBCOTM Life Technologies Ltd, Paisley, UK). Tumor cell viability was assessed in a hemo-cytometer after centrifugation at 1,000 g for 4 minutes, washing, re-suspension in PBS and addition of trypan blue. The cell suspension was adjusted to a density of 5×10^7 vital cells/ml for subpleural injection [4].

Anesthesia. Animals were anesthetized by intraperitoneal injection of pentobarbital sodium (50 mg/kg) followed by oro-tracheal intubation and ventilation with a standard rodent ventilator (Model 683, Harvard Apparatus, Les Ulis, France) with a mixture of oxygen and isofluran (0.5–2%), a tidal volume of 10 ml/kg with a positive end expiratory pressure (PEEP) of 2–3 cmH_2O, and a respiratory rate of 75–90/minutes. Postoperative analgesia consised of subcutaneous administration of 0.05 mg/kg Buphrenorfine® before extubation and then twice a day for 3 days after surgery.

Subpleural tumor generation in the left lower lung lobe. The animals were anesthetized and a left-sided mini-thoracotomy (7th intercostal space) was performed with subpleural injection of 0.1 ml tumor cell solution into the left lower lobe followed by closure of the thoracotomy and extubation [3].

Intraoperative photo-induction of the tumor-bearing lungs. After anesthesia a left-sided thoracotomy was performed through the 4th intercostal space with division of the inferior pulmonary ligament and mobilization of the left lung containing the subpleural tumor. The left external jugular vein was cannulated and 0.0625 mg/kg Visudyne® (Novartis, Hettlingen, Switzerland), dissolved in NaCl 0.9% and glucose 5% was injected. After a drug/light interval of 15 minutes, 689 nm laser light (35 mW/cm^2, 10 J/cm^2) was delivered to the tumor and the lower lobe through an optical microlens fiber (Model FD; Medlight, Ecublens, Switzerland) with the incident laser beam centered on the tumor and a treatment spot of 30 mm diameter (treatment time 5 minutes). In previous studies using an identical set up and drug-light conditions, no thermal effect has been measured at the surface of the treated area [3]. The fluence rate and the fluence were measured in real-time by a previously described light dosimetry system [10,11]. During and after PDT, ventilation with a positive end expiratory pressure (PEEP) of 2–3 cmH_2O was maintained.

Intravenous administration of Lipoplatin®. Immediately after laser light delivery, 5 mg/kg Lipoplatin® was injected intravenously via the jugular vein. The circulation time of Lipoplatin® was 60 minutes with the lung ventilated with a PEEP of 2–3 cm H_2O.

Assessment of Lipoplatin® concentrations in tumor and lung tissues. After 60 minutes of Lipoplatin® circulation time, the tumor and normal tissue of the left lung were analyzed separately by use of Inductively

Coupled Plasma Mass Spectrometry (ICP-MS) as described below. After dissection and excision of the tumor, the lung was cut in three pieces corresponding to the upper, middle and lower part of the lung. The coefficient of variation (CV%) and the ratio between tumor and lower lobe Lipoplatin® concentration were determined for each animal [3].

Photo-induction Combined to Systemic Lipoplatin® Chemotherapy in Porcine Chest Cavities

Study design. Fifteen animals received IV Lipoplatin® chemotherapy at a dose of 5 mg/kg combined to Visudyne®-mediated intrapleural low-dose photodynamic therapy *via* video-assisted thoracic surgery (VATS) with the following treatment conditions: 0.0625 mg/kg Visudyne® IV; drug-light interval 15 minutes; light dose of 10 J/cm^2 at the apex and diaphragm and 30 J/cm^2 at the dorsal and ventral hilum. These drug-light conditions were chosen based on our previous studies with the 10 J/cm^2 being the optimal fluence for tumor but not normal vessel permeabilisation and the 30 J/cm^2 being the first fluence with a potential leakage effect on normal vessels [6]. Six animals received Lipoplatin® immediately after light delivery (Protocol I) and nine animals 90 minutes before light delivery (Protocol II). Three animals in group II were treated at identical treatment conditions but with two lasers. Three animals received Lipoplatin® and underwent VATS pleural biopsies but without photo-induction (controls).

Pleural biopsies for Lipoplatin® concentration measurements were harvested at 10 and 30 J/cm^2 regions before and at regular intervals up to 90 minutes after light delivery. The postoperative course of all animals was monitored for 7 days after surgery. At that time point, autopsy was performed with histology and Lipoplatin® concentration measurements performed in both chest cavities and various organs.

Animals and housing. Göttingen minipigs (Bern, Switzerland) weighting 20–25 kg were used and treated in accordance with the National Institute of Health "Guidelines for the Care and Use of Laboratory Animals" and the Local Ethical Committee of the University of Lausanne.

Intrapleural VATS photo-induction. Following intramuscular sedation with ketamine 5 mg/kg, xylasine 0.1 mg/kg and atropine 0.1 mg/kg, general anesthesia was induced with isoflurane 2% using an FiO_2 of 100%. Anesthesia was maintained with isoflurane at a minimal alveolar concentration of 1,5 supplemented with IV meloxicam 0,4 mg/kg and a transcutaneous fentanyl patch 50 mcg/h. Endotracheal intubation, using a 7.0 Malinkrodt tube (Mallinkrodt Medical, Athlone, Ireland) was performed after a 2.5 mg/kg IV bolus of propofol. A 5 ml endobronchial blocker (Cook Medical, Bjaevereskov, Denmark) was placed in the left main bronchus, using an ultra slim single-use videoscope (Ambu® aScope™ 3 Slim, Ballerup, Denmark), for lung separation and single lung ventilation (Datex Engstrom, Bromma, Sweden). Immediately after lung isolation the FiO_2 was reduced to 50% using an air/oxygen mixture, and the right lung was ventilated with a tidal volume of 6 ml/kg, a positive end expiratory pressure of 5 cm H_2O and a respiratory rate adjusted to keep expired CO_2 within normal limits (35–40 mmHg). A central venous line was inserted in the right jugular vein for Visudyne® and Lipoplatin® administration and for blood sampling. Rectal temperatures were measured continuously during the procedure and maintained at 37–38°C with a heating blanket. Arterial oxygen saturation, expired gases (O_2, CO_2, isoflurane) and temperature were monitored continuously.

After general anaesthesia and exclusion of the lung, a left-side video-assisted thoracoscopic surgery (VATS) approach was performed with two thoracoports at the 6th and 7th intercostal space, respectively. Four 0.8 mm diameter isotopic probes (Model IP; Medlight, Ecublens, Switzerland) were inserted for real-time *in situ* light dosimetry and placed under endoscopic vision at different locations of the cavity (ventral hilar/dorsal hilar/apical/diaphragmatic). A dose of 0.0625 mg/kg Visudyne® was then IV administrated. After a drug-light interval of 15 minutes, illumination of the chest cavity with laser light at 689 nm and non-thermal fluence rates (typical average value of 35 mW/cm^2) was performed by use of one or two spherical light distributors (Model SD; Medlight, Ecublens, Switzerland) coupled to one or two diode lasers, respectively. The light distributor was inserted into one or two a sterile, commercially available intubation tubes filled with saline solution which were brought into the chest cavity though aexisting thoracoports. These light distributors were connected to laser diodes emitting at 690 nm (Ceralas PDT, 690/4–5 W/$\pm$3 nm/400 μm, Ceram-Optec GmbH, Bonn, Germany). Light delivery was guided by *in situ* light dosimetry and on-line measurements of the fluence and fluence rate at each of the four localisations within the chest cavity until each of the four probes had recorded a cumulated fluence of 10 J/cm^2 (apical/diaphragmatic) and 30 J/cm^2 (ventral hilar/dorsal hilar), respectively [10,11]. This setup designed to measure *in vivo* the fluence and fluence rate simultaneously and at several locations is based on the integration of a commercially available multichannel (up to 12 channels) power meter (model OP710 SI; OptoTest Corp. Camarillo, CA) equipped with isotropic detectors (Model IP; Medlight SA, Ecublens, Switzerland) with a standard laptop. This system was customized in the sense that the silicon photodiodes integrated in the setup were replaced with diodes with an optimized spectral sensitivity for the detection of light 690 nm. A homemade program written in C++/cli (Studzinski Médias & Electronique, Lausanne, Switzerland) was developed to operate this power meter, and to process and display the data.

Blood samples and pleural biopsies were harvested for Lipoplatin® concentration measurements in the 10 J/cm^2 and 30 J/cm^2 regions before and at 10 minutes intervals up to 90 minutes after light delivery. At that time point, the thoracoports were removed, a chest tube was inserted and extubation was performed. At the end of the procedure, the

insertions were closed in layers after introduction of a chest tube (16 gauge). Extubation was performed following ventilation with room air with continued PEEP and the chest tube was removed. Before waking up the animals, IV paracetamol (15 mg/kg) and meloxicam (0.4 mg/kg) were administered for postoperative analgesia.

Systemic Lipoplatin® administration. Lipoplatin® was administered IV at a dose of 5 mg/kg as perfusion over 5 minutes in anesthetized animals through the cannulated jugular vein. In protocol I, it was administered immediately after light delivery, in protocol II 90 minutes before light delivery. The two treatment protocols were chosen to examine whether different Lipoplatin® circulation times may influence the photo-induced permeabilisation effect on normal organs.

Assessment of lipoplatin® concentrations in blood and tissue samples. Blood samples (2 ml) and pleural biopsies of 10 and 30 J/cm^2 regions were harvested for Lipoplatin® concentration measurements before and at 10 minutes intervals up to 90 min after light delivery by use of inductively coupled mass spectrometry (IC-MS). All samples were stored at −80°C.

Follow-up. After extubation, the animals were observed for 7 days at the farm under supervision of a veterinary. Eating behavior, breathing frequency, wound healing, and treatment-related side effects were recorded.

Assessment of treatment-related toxicity. At day seven following surgery, autopsy was performed with histological assessment and Lipoplatin® concentration measurements of various organs. After euthanasia with pentobarbital 100 mg/kg, a sterno-laparotomy was performed and both chest cavities were inspected. Biopsies of the pleura, lung diaphragm, aorta, heart, liver, kidney, and skin were performed and processed for histological/ICP-MS analysis. Histological examination of the slices stained with haematoxylin and eosin (H&E) was performed by a blinded pathologist.

Assessment of Lipoplatin® Concentrations by Inductively Coupled Plasma Mass Spectrometry

The weight of tissue aliquot to be assayed for platinum was comprised between 50 and 300 mg. A volume of 500 mL of nitric acid 5M was added to tissue aliquot, and the obtained suspension was heated at 60°C overnight in a water bath. After *ca* 16 hours of mineralisation, the resulting yellow suspension containing solid tissue residues was sonificated for 30 seconds. A volume of 4.8 mL of nitric acid 2% was then added, and the resulting tissular suspension was subjected to a second sonification for 30 seconds. The homogeneous tissue suspension was finally centrifuged at 2,000*g* for 10 minutes. A 5 mL-volume of clear pale yellow supernatant was available for the assay of platinum by Inductively Coupled Plasma Mass Spectrometry (ICP-MS). A double focusing reverse geometry mass spectrometer was used (FinniganTM Element2 High Performance High Resolution ICP-MS instrument). The mass resolution was set to 500 in order to take advantage of the high signal transmission used in the low-resolution mode to increase the analytical sensitivity of Pt isotopes. The Element2 instrument was used with a standard glass spray chamber and Meinhard nebulizer. Calibration standards were prepared through successive dilutions using blank tissues solution, of 1 mg l^{-1} ICPMS stock solution (Bernd Kraft). Suprapur® grade nitric acid (65% Merck) was used for the preparation of standards (2+1000) and the dilution of samples. Ultrapure water was produced using Milli-Q® Ultrapure Water System (Millipore, Bedford). Rh was used as Internal Standard for samples and standards to correct signal drift. 100 µl of 100 µg l^{-1} Rh stock solution were added to 10 ml of standards and samples.

Statistical Analysis

Photo-induction on rodent lung tumors. Lipoplatin® concentrations in tumors and normal lung parenchyma of rodents and in blood and tissue samples of minipigs were compared using a two-tailed Student *t*-test for unrelated samples. The same holds true for the comparison of the ratio between tumor and normal lung drug uptake. The coefficient of variation in Lipoplatin® lung tissue levels was determined using the drug concentration in the three locations of treated lungs and compared using the Student's *t*-test. A bidirectional hypothesis was applied and significance was considered with $P < 0.05$.

Intrapleural photo-induction on minipigs. Lipoplatin® concentrations in blood and tissue samples with and without photo-induction were compared using the Student *t*-test for unrelated samples. A bidirectional hypothesis was applied and significance was considered with $P < 0.05$.

RESULTS

Photo- Induction Combined to Systemic Lipoplatin® Chemotherapy on Lung Tumors

Lipoplatin concentrations in tumors and normal lung tissues. Table 1 shows the Lipoplatin® concentrations in adenocarcinoma, sarcoma and mesothelioma tumors as well as in the surrounding normal lung tissue, with and without PDT pre-treatment. Photo-induction enhanced Lipoplatin® uptake in all three tumor types and significantly increased the ratio between tumor and lung drug concentrations in sarcoma ($P = 0.0008$) and adenocarcinoma ($P = 0.01$) but not mesothelioma, compared to IV drug administration alone. The coefficient of variation (CV%) of Lipoplatin® concentrations in the three parts of the lungs did not differ significantly between treatment groups indicating a homogeneous Lipoplatin® distribution in the lungs for all treatment groups, including those with photo-induction.

Intrapleural Vats Photo-induction Combined to Systemic Lipoplatin® in Porcine Chest Cavities

Light delivery. The analysis of the on-line measured and computer-stored fluences during light delivery

TABLE 1. Lipoplatin Concentration in Tumors and Lower Lobe of Rodent Lungs (mean ± SD) After IV Lipoplatin® Administration (5 mg/kg), With and Without Visudyne®-Mediated Photo-Induction (10 J/cm²)

	n	Tumor (ng/mg)	Lower Lobe (ng/mg)	Ratio[a]	CV (%)[b]	*P* value[c]
Sarcoma						
Lipoplatin® + PDT	7	2.7 ± 0.8	3.3 ± 1.0	0.8 ± 0.1	34.2	0.0008
Lipoplatin®	7	2.3 ± 1.4	3.9 ± 2.1	0.6 ± 0.1	54.6	
Adenocarcinoma						
Lipoplatin® + PDT	7	3.2 ± 0.8	2.3 ± 0.5	1.4 ± 0.4	32.6	0.016
Lipoplatin®	7	2.4 ± 0.3	2.7 ± 0.5	0.9 ± 0.1	23.2	
Mesothelioma						
Lipoplatin®+ PDT	6	2.9 ± 0.9	3.2 ± 1.2	0.9 ± 0.2	33.2	0.5
Lipoplatin®	6	2.3 ± 0.6	2.6 ± 0.4	0.9 ± 0.1	24.3	

[a]Ratio of Lipoplatin® concentration between tumor and normal surrounding lung tissue (median/range).
[b]Coefficient of variation of Lipoplatin® uptake in three different parts of the treated lung.
[c]*P* values between ratios of tumor to normal lung Lipoplatin® concentrations, with and without photo-induction.

revealed a homogeneous illumination of the chest cavity with appropriate cumulated fluences at the different locations for both modes of illumination (one vs. two lasers, Fig. 1a). The mean time to obtain 10 J on the apex/diaphragm and 30 J in the hilar region were homogenous and reported in Fig. 1b. The mean illumination time to obtain the required light dose at different locations was shorter when using two lasers compared to one (27.6 ± 19 vs. 8.5 ± 1 minutes to obtain 10 J/cm2 to the chest cavity using one or two lasers, respectively, Fig. 1c).

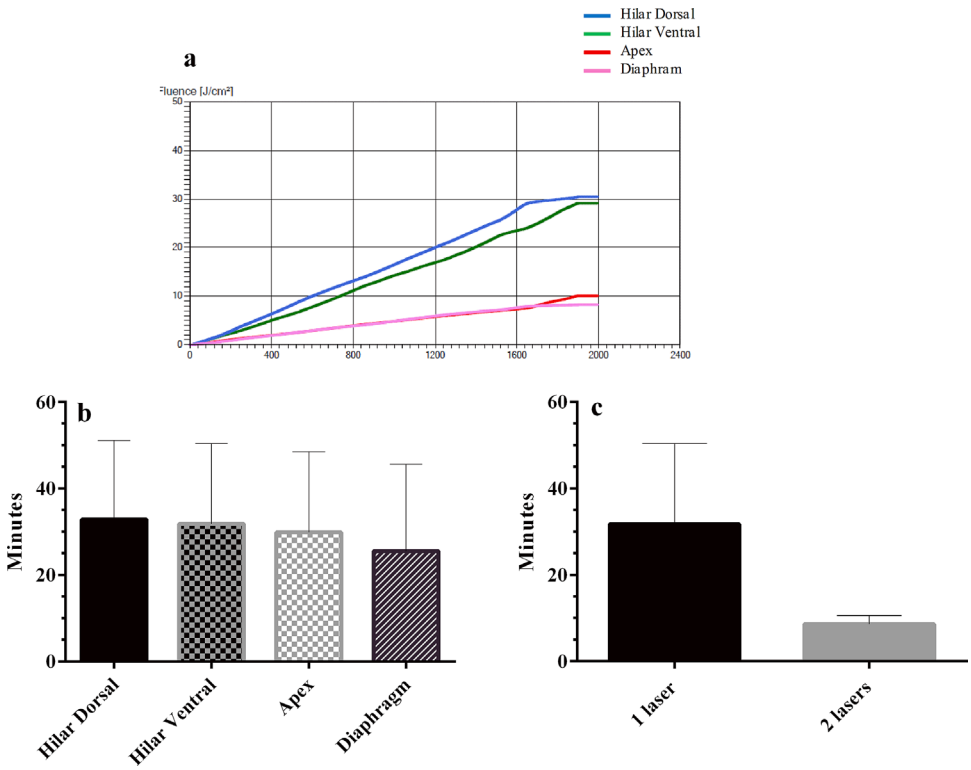

Fig. 1. Laser light delivery in the chest cavities of minipigs during photo-induction: (**a**), real-time measurement of the cumulative fluence applied to the four locations of the chest cavity in one of the animals from our experiment; (**b**), time interval (minutes, mean ± SD) of illumination in order to reach the defined cumulative fluence at different locations in the chest cavities during photo-induction (10 J/cm² to apex and the diaphragm, 30 J/cm² to the ventral and dorsal hilum, $n = 12$); (**c**), time interval (minutes, mean ± SD) of illumination to reach the required cumulative fluence within the chest cavities using one ($n = 12$) or two lasers ($n = 3$).

Lipoplatin® concentration measurements in blood and tissue. For both treatment protocols, the Lipoplatin® concentrations were assessed in blood and in pleural biopsies in the 10 J and 30 J/cm^2 treated regions before and at 10 minutes intervals up to 90 minutes following photo-induction. Also, Lipoplatin concentrations in blood and in various organs of the operated and non-operated sides were assessed 7 days after surgery. In protocol I, the Lipoplatin® concentrations in pleural biopsies reached a plateau value 10 minutes after light delivery without significant differences between the 10 J and 30 J/cm^2 locations and between animals with and without photo-induction (Fig. 2a). The assessment of blood Lipoplatin® concentration revealed a similar kinetic to that observed in tissues (Fig. 2b). The pleura Lipoplatin® concentrations assessed 10 minutes after light delivery were significantly higher for treatment protocol I compared to II (2.37 ± 0.7 ng/mg vs. 1.37 ± 0.7 ng/mg, $P = 0.001$, Fig. 3a). The same holds true for blood Lipoplatin® concentrations (25.22 ± 13 ng/ml vs. 7.04 ± 2.2 ng/ml, $P = 0.003$, Fig. 3b). At day 7, Lipoplatin® concentrations were not significantly different between animals pre-treated or not by photoinduction except for lung tissues on the operated side: Control animals had a higher Lipoplatin® lung uptake compared to the contralateral lung (controls) and to animals treated by photo-induction ($P < 0.05$, Fig. 4).

Toxicity and feasibility. The procedure was well tolerated in all animals without relevant side effects, intrapleural or chest wall infections, or toxicity. All animals showed a normal eating behavior and stable weight up to 7 days following surgery with no skin phototoxicity which was specifically assessed at the site of surgery and the site of pulse oxymetry measurement (left ear) during and 7 days after the procedure.

Tissue injury. An autopsy was performed in all animals 7 days after the intervention. Macroscopic and histological analysis revealed no abnormality or injury apart from discrete and localized pleural adhesions within the operated chest cavity. Histological assessment did not reveal injuries of intrathoracic organs; there were no differences in histology of lung, pleura, diaphragm, heart, and great vessels between the operated vs contralateral chest cavities or between animals with and without photo-induction (Fig. 5). The same holds true for histological analyses of liver, kidney and skin. Also, the use of one versus two lasers had no effect on the macroscopic and histological assessment of intrathoracic organs.

DISCUSSION

Photodynamic therapy (PDT) has emerged as an attractive cytotoxic treatment modality for superficially growing tumors [12]. It was tested in the clinics for a variety of malignancies including malignant pleural diseases [13–20] but had important side effects and toxicity when large surfaces were treated [14,21]. The dominant mechanism of action of conventional PDT is the local generation of singlet oxygen, which results in the destruction of tumor cells and of tumor microvasculature [12]. However, it has been shown with lower drug light conditions that PDT could cause a variety of vascular effects ranging from a transient vasospasm to vessel transport enhancement and vessel wall disintegration with thrombosis [22–26]. Scientific interest, so far, was mainly focused on the vessel-occlusive effects of PDT while its vessel transport enhancement properties have only recently been explored to improve the uptake and efficacy of systemically administered cytostatics to tumors. In contrast to conventional PDT which aims to obtain tumor ablation by a shutdown of tumor vasculature or a cytotoxic effect on tumor cells, this new PDT application requires specific vessel-targeted photosensitizers, a short drug-light interval to keep the sensitizer intravascular and lower drug/light conditions than generally used for standard PDT treatments. Recently, several studies have explored low-dose PDT to enhance the transfer of macromolecular cytostatic agents across the endothelial barrier into the tumor interstitium [2–6]. These studies have shown that PDT pre-treatment at low drug-light conditions and using vessel targeted sensitizers such as Visudyne® could enhance the uptake and distribution of systemically administered macromolecular cytostatics in tumors while sparing the normal surrounding tissues (a phenomenon called photo-induction). By facilitating the tumor uptake of systemically administered chemotherapy, photo-induction may contribute to control malignant pleural deposits while avoiding the adverse effects of conventional PDT on surrounding structures.

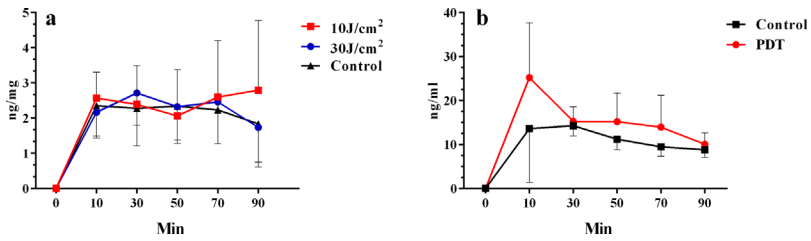

Fig. 2. Lipoplatin® concentrations (**a**), in pleural biopsies at 10 J and 30 J/cm^2 locations, and (**b**), in blood before and at different time intervals following light delivery (mean ± SD) using protocol I (Lipoplatin® injection immediately after light delivery, $n = 6$). Controls animals ($n = 3$) received VATS and Lipoplatin® but no photo-induction.

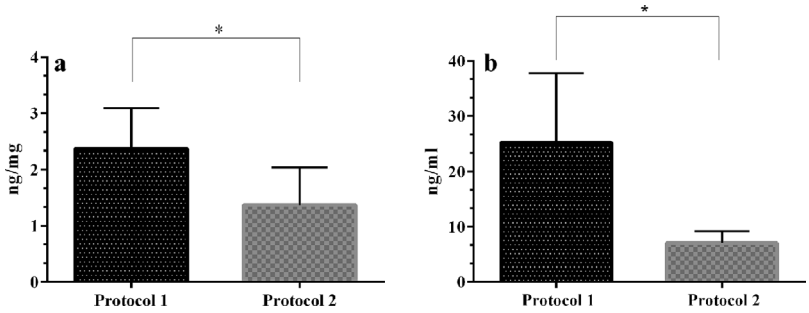

Fig. 3. Lipoplatin® concentrations (mean ± SD) in (**a**), pleural biopsies and (**b**), blood 10 minutes after light delivery for treatment protocol I (Lipoplatin® injection immediately after light delivery, $n = 6$) and protocol II (Lipoplatin® injection 90 minutes before light delivery, $n = 9$), respectively (*: $P < 0.05$ between Lipoplatin concentrations in the pleura and blood between protocols I and II).

In previous experiments, we have shown that Visudyne®-mediated photo-induction resulted in a significant increase of liposomal doxorubicin uptake in mesothelioma, adenocarcinoma, and sarcoma tumors on rodent lungs but that the extent of tumor drug uptake paralleled tumor vessel density [4]. Regarding drug-light conditions, Visudyne® was used as sensitizer and administered at half of the dose recommended in patients (0.0625 mg/kg) [27], a short drug-light interval (15 minutes) to keep the sensitizer intravascular and a low fluence (10 J/cm^2). This fluence value was based on a previous studies performed in H-Meso1 tumors grown in dorsal skinfold chambers [6]. In this model, we found that a fluence of 10 J/cm^2 was optimal to enhance vascular transport of macromolecules in tumors while leaving normal tissues unaffected; a higher light dose, however, resulted in tumor vessel occlusion which impeded tumor drug transfer [6]. Using these optimized drug-light conditions for the treatment of mesothelioma xenografts in nude mice, we determined tumor response following Visudyne®-mediated photo-induction combined to Lipoplatin®, a macromolecular liposomal formulation of cisplatin, currently used in clinical phase II and III trials [7–9]. We observed a significant tumor growth delay after photo-induction combined to systemic chemotherapy compared to Lipoplatin® chemotherapy alone, without evidence of tumor re-growth up to 28 days after treatment [6].

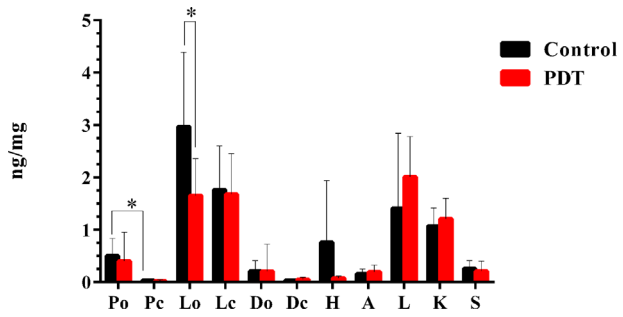

Fig. 4. Lipoplatin® concentrations (mean ± SD) in different organs 7 days after photo-induction (P, pleura; L, lung; D, diaphragm; H, heart; L, liver; K, kidney; S, skin; O, operated chest; C, contralateral; non operated chest) in controls ($n = 3$) and animals with photo-induction ($n = 15$).

The precise mechanism on how photo-induction enhances effective permeability of tumor vessels for macromolecular cytostatics is still unknown. Interestingly, effective permeability of tumor vessels and subsequent drug distribution do not necessarily correspond to the intrinsic vessel permeability. For example, it was well demonstrated that solid tumors have wide networks of neovessels which are permeable and cause interstitial fluid pressure (IFP) to be high [28]. Macromolecular therapeutics are known to depend on vascular convection for their extravasation between the intra- and extra-vascular spaces [28] which rely on tumor hydrostatic and oncotic pressures. The increased IFP associated with the high vascular permeability of tumor neovessels hinders convection and drug delivery [28]. We have recently shown on rodent lung tumors that photo-induction could cause a transient drop in tumor but not normal tissue IFP while keeping tumor blood flow constant which may explain enhanced drug convection from the intravasal space into tumors and a subsequent increase in tumor drug uptake [5].

This preclinical study was undertaken to assess intrapleural Visudyne®-mediated photo-induction combined to liposomal cisplatin (Lipoplatin®) as a pathway to increase the uptake and distribution of approved, cisplatin-based chemotherapy in pleural tumors and thereby improve outcome. This is potentially an attractive treatment concept for superficially spreading chemo-resistant pleural malignancies and may be considered in patients referred for the thoracoscopic treatment of malignant pleural effusion. It has a significant therapeutic potential for a frequently encountered situation for which at present there in no efficient therapy available. Our results indicate that photo-induction selectively increased the tumor uptake of subsequently IV administered Lipoplatin® on sarcoma, adenocarcinoma, and mesothelioma grown subpleurally on rodent lungs. These results corroborate with previous findings using the same model and photo-induction conditions but liposomal doxorubicin: Sarcoma and adenocarcinoma revealed a better tumor drug uptake than mesothelioma which may be explained by a lower tumor vessel density for this tumor type [4].

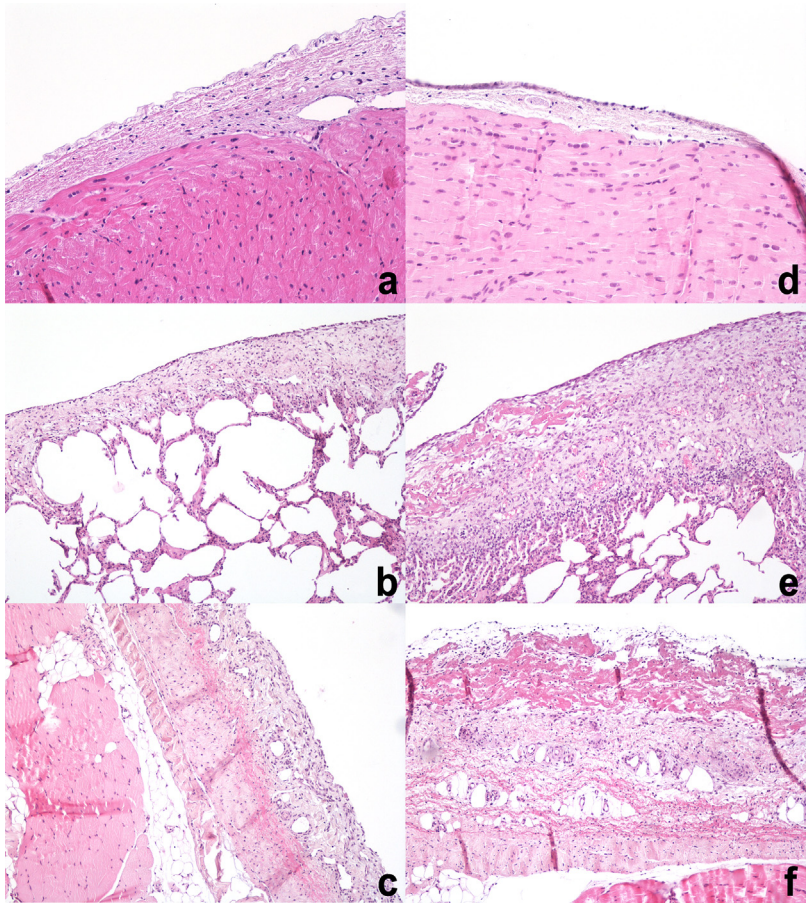

Fig. 5. Histological assessment of intrathoracic organs at day 7 after operation: (**a**), heart; (**b**), lung; and (**c**), diaphragm after Lipoplatin® administration and photo-induction (2 lasers) without evident histological lesions except for discrete fibrinous reaction on the pleural surface; (**d**), heart; (**e**), lung; and (**f**), diaphragm of a control animal without evident histological lesions except for discrete fibrinous reaction on the pleural surface (H&E × 100).

In the second part of our experiments and with identical treatment parameters, we investigated intrapleural photo-induction combined to systemic administration of Lipoplatin® in tumor free minipigs as a safety and feasibility assessment. For this purpose, we used a CE certified and customized device for clinical applications under sterile conditions which has been developed for intrapleural PDT and assessed in previous experiments in rodent and porcine chest cavities [10,11]. It consists of a diode laser emitting a sensitizer-specific wavelength coupled to an optical fiber-based light distributor for endoscopic treatment, customised for applications in operation theatres. Four isotropic optical fibres coupled to a multichannel powermeter allowed for *in situ,* real-time monitoring of fluence rates and fluences at different locations within the chest cavity during illumination. This set up was installed through a classical video-assisted thoracoscopic setup used for conventional pleural biopsy or talcage in patients. It allowed the homogenous delivery of controlled light doses within the complex geometry of the chest cavity. A similar set-up is currently used for patients undergoing surgery and conventional intraoperative PDT for mesothelioma [19,20].

The results of intrapleural photo-induction of porcine chest cavities combined to IV Lipoplatin chemotherapy indicate that this treatment is feasible and well tolerated. With two lasers, the mean illumination time to deliver a cumulative fluence of 10 J/cm^2 to the entire chest cavity was only of approximately 8.5 minutes. We observed no perioperative or postoperative complications including skin phototoxicity up to 7 days after the proceedure. This was confirmed by histological examination of most organs 7 days after treatment. The Lipoplatin® concentration in pleura biopsies reached a plateau approximately 10 minutes after drug administration and was significantly higher with protocol I compared to protocol II. This may be explained by the pharmacokinetic profile of Lipoplatin® and its redistribution pattern over time following IV injection. It does not seem to be related to a photo-induction effect. However, for both treatment schemes, there were no differences in drug tissue concentrations between the 10 J and 30 J/cm^2 locations suggesting that the combination of different Lipoplatin® circulation times and fluences did not lead to normal vessel leakage and subsequent accumulation of cytotoxic drugs at inappropriate sites.

Our study has several limitations. First, the tumor model used did not rely on a pleural growing tumor but rather on a syngeneic subpleural tumor model. This specificity of our model could affect blood supply and chemotherapeutic drug delivery which could affect our results. Thus, caution is required in the interpretation of our results. However, our model does allow uniform tumor growth with comparable tumor sizes and volumes which facilitates the comparison of the Lipoplatin® uptake following a standardized photo-induction regimen. Second, the use of single lung ventilation during photo-induction may alter the blood flow, local tissue oxygenation, and interfere with drug uptake. Lung collapse causes local hypoxia which has a vasospastic effect on the pulmonary vasculature [30]. The latter has been previously shown to cause heterogeneity in lung perfusion [31]. In addition, oxygen levels and vascular perfusion are important factors that can influence the photodynamic therapy effect on vessels [2]. In our study, we observed an increase in Lipoplatin® uptake in the non-ventilated lung on the operated side compared to the controlateral lung, but only in control animals. Interestingly, Lipoplatin® uptake in the operated lung was decreased following photo-induction compared to controls. The interpretation of this data is difficult given the small number of animals of our control group. However, as Lipoplatin® blood concentration had reached a steady state in blood (injected before lung exclusion), it could be that hypoxemic vasoconstriction improved tissue drug uptake though an enhancement of diffusion. On the other hand, photo-induction, which also leads to microvascular alterations in the lung, might interfere with these potential mechanisms and explain the difference between drug uptake in control vs photoinduced lungs. Third, we have not formerly excluded a hyperthermic effect on the pleural cavity in our porcine model (no temperature measurement on the chest performed during photoinduction). However, the light fluence and fluence rates used in our study are several orders of magnitude lower to those recommended for Visudyne®-mediated PDT in the field of ophthalmology where the avoidance of a hyperthermic effect is mandatory. Also the animal temperature monitoring was mostly on the hypothermic side with the requirement of a heating blanket during the procedure which excludes an important hyperthermic effect. Forth, the laser light penetration has not been fully assessed in our models. We found that 4 mm tumors in the rat could respond to photoinduction with enhanced Lipoplatin uptake. We have also found in previous studies that transcutaneous application of laser lead to better Lipoplatin uptake and tumor response in 5 mm mesothelioma tumors grown subcutaneously in mice [6]. Also, based on the literature, our light conditions should allow a penetration of at least 5 mm which should be sufficient to treat thin tumor deposits that are generally observed in malignant pleural effusion in the clinics [29].

In conclusion, our experiments suggest that: i) Visudyne®-mediated photo-induction with 10 J/cm^2 selectively increases the uptake of systemic liposomal cisplatin (Lipoplatin®) in various pleural tumors grown orthotopically on rodent lungs (proof of concept); and ii) intrapleural video-assisted thoracoscopic (VATS) photo-induction of chest cavities combined to systemic Lipoplatin® chemotherapy is feasible and well tolerated in minipigs, with homogenous delivery of 10 J/cm^2 using a customised equipment for applications under sterile conditions in the operation room. Based on these encouraging findings, we plan to perform a clinical phase I trial that will explore VATS intrapleural photo-induction as a mean to improve the uptake and distribution of Lipoplatin® in selected patients with pleural malignancies.

ACKNOWLEDGMENTS

We would like to thank Mr Burki and Pavillard for their help with the animal experiments.

REFERENCES

1. Statement of the american thoracic society: Management of malignant pleural effusions. Am J Respir Crit Care Med 2000;162:1987–2001.
2. Snyder JW, Greco WR, Bellnier DA, Vaughan L, Henderson BW. Photodynamic therapy: A means to enhanced drug delivery to tumors. Cancer Res 2003;63:8126–8131.
3. Cheng C, Debefve E, Haouala A, Andrejevic-Blant S, Krueger T, Ballini JP, et al. Photodynamic therapy selectively enhances liposomal doxorubicin uptake in sarcoma tumors to rodent lungs. Lasers Surg Med 2010;42:391–399.
4. Wang Y, Gonzalez M, Cheng C, Haouala A, Krueger T, Peters S, et al. Photodynamic induced uptake of liposomal doxorubicin to rat lung tumors parallels tumor vascular density. Lasers Surg Med 2012;44:318–324.
5. Perentes JY, Wang Y, Wang X, Abdelnour E, Gonzalez M, Decosterd L, Wagnieres G, van den Bergh H, Peters S, Ris HB, Krueger T. Low-dose vascular photodynamic therapy decreases tumour interstitial fluid pressure, which promotes liposomal doxorubicin distribution in a murine sarcoma metastasis model. Transl Oncol 2014;7:393–399.
6. Wang Y, Wang X, Le Bitoux MA, Wagnieres G, Vandenbergh H, Gonzalez M, Ris HB, Perentes JY, Krueger T. Fluence plays a critical role on the subsequent distribution of chemotherapy and tumor growth delay in murine mesothelioma xenografts pre-treated by photodynamic therapy. Lasers Surg Med 2015;47:323–330.
7. Boulikas T. Clinical overview on Lipoplatin: A successful liposomal formulation of cisplatin. Expert Opin Investig Drugs 2009;18:1197–1218.
8. Stathopoulos GP, Boulikas T, Vougiouka M, Deliconstantinos G, Rigatos S, Darli E, Viliotou V, Stathopoulos JG. Pharmacokinetics and adverse reactions of a new liposomal cisplatin (Lipoplatin): Phase I study. Oncol Rep 2005;13:589–595.
9. Stathopoulos GP, Antoniou D, Dimitroulis J, Stathopoulos J, Marosis K, Michalopoulou P. Comparison of liposomal cisplatin versus cisplatin in non-squamous cell non-small-cell lung cancer. Cancer Chemother Pharmacol 2011;68:945–950.
10. Krueger T, Altermatt HJ, Mettler D, Scholl B, Magnusson L, Ris HB. Experimental photodynamic therapy for malignant pleural mesothelioma with pegylated mTHPC. Lasers Surg Med 2003;32:61–68.
11. Krueger T, Pan Y, Tran N, Altermatt HJ, Opitz I, Ris HB. Intraoperative photodynamic therapy of the chest cavity in malignant pleural mesothelioma bearing rats. Lasers Surg Med 2005;37:271–277.
12. Henderson BW, Gollnick SO. Mechanistic principles of photodynamic therapy. In: Vo-Dinh T (ed), Biomedical Photonics Handbook, Boca Raton: CRC Press, 2003. pp 36-1–36-27.
13. Ris HB, Altermatt HJ, Inderbitzi R, Hess R, Nachbur B, Stewart JC, Wang Q, Lim CK, Bonnett R, Berenbaum MC. Photodynamic therapy with chlorins for diffuse malignant mesothelioma: Initial clinical results. Br J Cancer 1991;64:1116–1120.

14. Ris HB, Altermatt HJ, Nachbur B, Stewart CM, Wang Q, Lim CK, Bonnett R, Althaus U. Intraoperative photodynamic therapy with m-tetrahydroxyphenylchlorin for chest malignancies. Lasers Surg Med 1996;18:39–45.
15. Takita H, Mang TS, Loewen GM, Antkowiak JG, Raghavan D, Grajek JR, Dougherty TJ. Operation and intracavitary photodynamic therapy for malignant pleural mesothelioma: a phase II study. Ann Thorac Surg 1994;58:995–998.
16. Baas P, Murrer L, Zoetmulder FA, Stewart FA, Ris HB, van Zandwijk N, Peterse JL, Rutgers EJ. Photodynamic therapy as adjuvant therapy in surgically treated pleural malignancies. Br J Cancer 1997;76:819–826.
17. Pass HI, Temeck BK, Kranda K, Thomas G, Russo A, Smith P, Friauf W, Steinberg SM. Phase III randomized trial of surgery with or without intraoperative photodynamic therapy and postoperative immunochemotherapy for malignant pleural mesothelioma. Ann Surg Oncol 1997;4:628–633.
18. Moskal TL, Dougherty TJ, Urschel JD, Antkowiak JG, Regal AM, Driscoll DL, Takita H. Operation and photodynamic therapy for pleural mesothelioma: 6-year follow-up. Ann Thorac Surg 1998;66:1128–1133.
19. Friedberg JS, Mick R, Stevenson J, Metz J, Zhu T, Buyske J, Sterman DH, Pass HI, Glatstein E, Hahn SM. A phase I study of Foscan-mediated photodynamic therapy and surgery in patients with mesothelioma. Ann Thorac Surg 2003;75: 952–959.
20. Friedberg JS, Culligan MJ, Mick R, Stevenson J, Hahn SM, Sterman D, Punekar S, Glatstein E, Cengel K. Radical pleurectomy and intraoperative photodynamic therapy for malignant pleural mesothelioma. Ann Thorac Surg 2012;93: 1658–1665.
21. Pelton J, Kowalyshyn M, Keller S. Intrathoracic organ injury associated with photodynamic therapy. J Thorac Cardiovasc Surg 1992;103:1218–1223.
22. Fingar VH. Vascular effects of photodynamic therapy. J Clin Laser Med Surg 1996;14:323–328.
23. Debefve E, Pegaz B, Ballini JP, Konan YN, Van den Bergh H. Combination therapy using aspirin enhanced photodynamic selective drug delivery. Vasc Pharmacol 2007;46:171–180.
24. Debefve E, Pegaz B, van den Bergh H, Wagnières G, Lange N, Ballini JP. Video monitoring of neovessel occlusion induced by photodynamic therapy with verteporfin (Visudyne), in the CAM model. Angiogenesis 2008;11:235–243.
25. Debefve E, Cheng C, Schaefer S, Yan H, Ballini JP, Van den Bergh H, lehr HA, Ruffiezx C, Ris HB, Krueger T. Visudyne-mediated photodynamic therapy enhances macromolecular delivery in normal tissue: Insights using intravital microscopy. J Photochem Photobiol B 2009;98:69–76.
26. Debefve E, Mithieux F, Perentes JY, Wang Y, Cheng C, Schaefer SC, Ruffieux C, Ballini JP, Gonzalez M, van den Bergh H, Ris HB, Lehr HA, Krueger T. Leukocyte-endothelial cell interaction is necessary for photodynamic therapy induced vascular permeabilization. Lasers Surg Med 2011;43:696–704.
27. Bessler N, Committee VSW. Verteporfin therapy in age-related macular degeneration: An open-label multicenter photodynamic study of 4435 patients. Retina 2004; 20:3–7.
28. Jain RK. Normalization of tumor vasculature: An emerging concept in antiangiogenic therapy. Science 2005;307:58–62.
29. Sandell J, Zhu TC. A review of in-vivo optical properties of human tissues and its impact on PDT. J Biophotonics 2011;4(11-12):773–787.
30. Porcelli R, Viau A, Demeny M, Naftchi NE, Bergofsky EH. Relation between hypoxic pulmonary vasoconstriction, its humoral mediators and alpha-beta adrenergic receptors. Chest 1977;71(2 suppl):249–251.
31. Krueger T, Kuemmerle A, Kosinski M, Denys A, Magnusson L, Stupp R, Delaloye AB, Klepetko W, Decosterd L, Ris HB, Dusmet M. Cytostatic lung perfusion results in heterogeneous spatial regional blood flow and drug distribution: Evaluation of different cytostatic lung perfusion techniques in a porcine model. J Thorac Cardiovasc Surg 2006;132(2):304–311.